Arch. Metall. Mater. **69** (2024), 3, 1231-1239

DOI: https://doi.org/10.24425/amm.2024.150946

D. CRISTISOR[1], D.-L. CHICET[2*], B. ISTRATE[1], C. STESCU[1], C. MUNTEANU[1,3*]

INFLUENCE OF TiO_2 ALLOYING PERCENTAGE ON THE MORPHOLOGY OF APS-DEPOSITED COATINGS FROM Cr_2O_3 POWDERS

In this paper we studied how alloying with different percentages of TiO_2 influences the microstructure of Cr_2O_3 base matrix coatings deposited by plasma spray (APS). Thus, five different types of coatings were made, in which the percentage of TiO_2 varied as 0%, 10%, 20%, 30% and 40%. The samples were analysed morphologically both on the surface and in cross-section using direct observation and electron microscopy (SEM). It was observed that none of the TiO_2-containing coatings is a simple blend of distinct phases, but are coatings with a specific layered lamellar structure, with coarser and smooth areas, depending on the Ti wt.% presence. All the coatings analysed show micro cracks, porosities and inhomogeneous structure, but with a higher density directly proportional to the percentage of TiO_2 in the composition of the coated powder.

Keyword: Cr_2O_3 – TiO_2 coatings; APS; microstructure morphology

1. Introduction

The thermal spray coatings produced from Cr_2O_3 powders are used for a wide range of applications that require abrasive and sliding wear resistance, including: papermaking rolls and blades, hydraulic seal joints, pump parts, shaft sleeves, seals, valves, components for high-speed automatic machinery such as packaging and food processing machinery [1]. Although these coatings show very good corrosion [2] and abrasion resistance properties and satisfactory hardness values, their applicability is limited by their brittleness [3]. For this reason, various materials have been investigated which, when added to the base material, improve the ductility and compactness of the coating, one of them being TiO_2 powder [4-6]. This study is part of a more complex study aimed at determining an optimal combination of Cr_2O_3 – TiO_2 powders that, deposited by atmospheric plasma spray, will improve the sliding wear behaviour of kingpin axles in the heavy-duty automotive industry.

Titanium oxide is a multifunctional powder with diverse uses, from medical technology [7] to gas sensor technology to photocatalytic or wear protection [8]. By thermal deposition, hard, dense, abrasion-resistant coatings with interfacial toughness and superior tensile adhesion strength [9] can be obtained from this type of powder, provided they are used at temperatures below 540°C. This temperature limit is imposed by the irreversible phase transformation (from the athanase to the rutile phase), which generates microcracks and exfoliation of the ceramic coating, which in any case has a low plasticity and resilience [10].

Chromium oxide powder is a very promising material for a wide range of industrial applications, as it can be deposited by various thermal spraying processes. This results in coatings with excellent wear and sliding friction properties being the most chemically inert of all oxides used in this application. Another advantage of this type of material is its operating temperature, which can exceed 540°C [11]. However, coatings made of Cr_2O_3 are associated with high brittleness, which influences its tribological behaviour, mainly due to its inhomogeneous structure [12]. For example, under sliding friction stresses, the coating is affected by different wear processes such as plastic deformation, adhesion and brittle fracture [6/10]. However, the wear resistance properties are superior to other hard coatings, such as WC-Co, Al_2O_3 or TiO_2 [13,14] under both wet and dry wear conditions [15,16].

However, these weaknesses can be mitigated by alloying Cr_2O_3-based powders with other chemical elements or oxide compounds, one example being TiO_2 doping, which can provide an increase in ductility, favoring the formation of denser coatings with lower roughness than pure Cr_2O_3 [17-19]. Titanium

[1] GHEORGHE ASACHI TECHNICAL UNIVERSITY OF IASI, DEPARTMENT OF MECHANICAL ENGINEERING, BLVD. MANGERON, NO. 61, 700050, IASI, ROMANIA
[2] GHEORGHE ASACHI TECHNICAL UNIVERSITY OF IASI, DEPARTMENT OF MATERIALS SCIENCE AND ENGINEERING, BLVD. MANGERON, NO. 41, 700050, IASI, ROMANIA
[3] TECHNICAL SCIENCES ACADEMY OF ROMANIA, 26 DACIA BLVD, BUCHAREST, 030167, ROMANIA

* Coressponding author: daniela-lucia.chicet@academic.tuiasi.ro

oxide has been shown to play an important role in increasing the strength and decreasing the porosity of the layer of which it is part by binding the other ceramic particles with which it is mixed [d/20]. Thus, by combining different percentages of TiO_2, coatings characterized by very good abrasion, heat and corrosion resistance combined with very good fracture toughness for the ceramic coatings category are obtained.

2. Materials and methods

In order to study how the TiO_2 alloying percent influences the microstructure of a Cr_2O_3 base matrix coating deposited by plasma spray (APS), two type of powders commercially available were acquired from market: Amdry 6415 (99%wt. Cr_2O_3, fused sintered and crushed) and Metco 6483 (Cr_2O_3 40 TiO_2, blended). Their morphology, acquired by scanning electron microscopy is presented in Fig. 1.

In order to modify the alloying percent, there were calculated and measured by weighing on an electronic balance the quantities needed to obtain a 10 wt.%, 20 wt.% and 30 wt.% alloying with TiO_2 by mechanically mixing the 99%wt. Cr_2O_3 powder with the Cr_2O_3 40 TiO_2. The Nominal Particle Size Distribution is (–15 +5) μm for Cr_2O_3 powder and (– 90 +16) μm for Cr_2O_3-40TiO_2, both of them with an angular / blocky morphology.

The mixing of the two types of powder was carried out in a hermetically sealed glass container by mechanical stirring in a dry environment for 2 minutes. The most important condition was to keep the powders dry before and after mixing by introducing desiccant materials into the containers used for mixing and subsequent storage.

The SprayWizard 9MCE Facility (Metco-Oerlikon, 2006) was used for the thermal spraying, with the following parameters: voltage – 58.8 V, intensity – 496 A, primary gas flow (argon) – 60 NLPM, secondary gas flow (hydrogen) – 45 NLPM, powder feed rate – 60 gr/minute, stand-off distance – 80 mm.

For the substrate, rectangular profiles (60×30×5 mm) made of low-alloy steel (see TABLE 1) was chosen, from which the studied samples were cut. The surface of each sample was prepared by sand-blasting with the purpose of cleaning all the impurities and to activate it by texturing. In order to ensure the reproducibility of the experiment, three samples of each type of deposited coating were produced.

TABLE 1

Chemical composition of the steel substrate according EN 10025-2/2004

Chemical element %wt.	C	Mn	P	S	N	Cu
Steel substrate	max 0.17	max 1.4	max 0.035	max 0.035	max 0.12	max 0.55

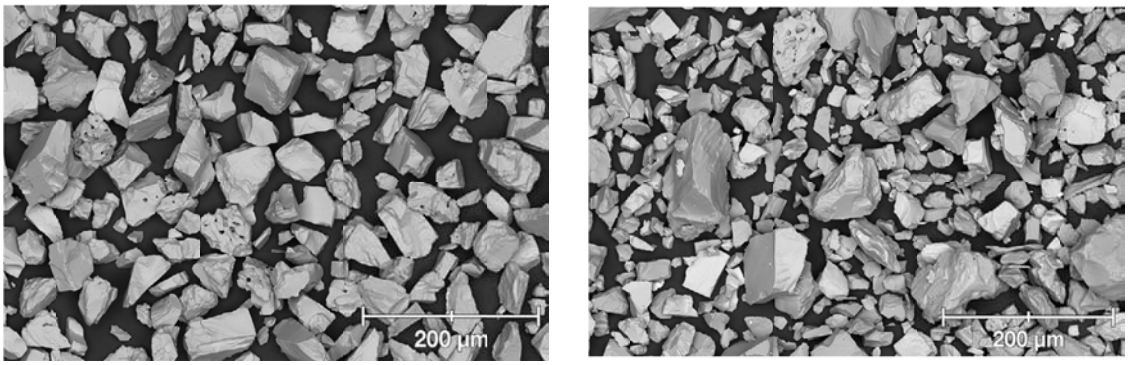

a) b)

Fig. 1. Secondary electron image (SEI) of the base – powders: a) Cr_2O_3, b) Cr_2O_3 – 40TiO_2

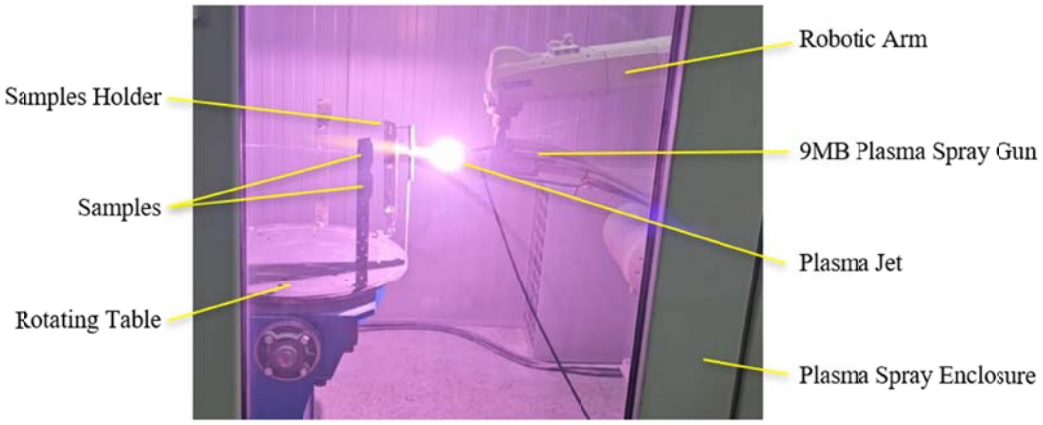

Fig. 2. Aspect during the Plasma Spray procedure

For the analysis of the morphology of the coatings, the classical methods of analysis were used: direct observation and electron microscopy, the latter being the most used, being carried out with the Vega Tescan LMH2II electron microscope, on the High Vacuum module, with a filament voltage of 30 kV and ETD detector for the Secondary Electron Images (SEI). This was complemented by semi-quantitative elemental chemical analysis carried out by the EDS (Energy-dispersive X-ray spectroscopy) method, using the Brucker analysis module, with which the electron microscope is equipped.

3. Results and discussion

3.1. Morphological analysis

After the samples were made by plasma spraying, they were visually analysed and no visible cracks, delaminations or exfoliation were observed in any of the five samples. For the analysis of the coating morphology, a representative sample from each batch was taken and observed by electron microscopy, the images obtained being shown for each type of sample in Figs. 3-7.

Coatings deposited by plasma spraying are created when a stream of particles strikes the substrates and the resulting structure depends on several factors such as temperature, velocity and particle size distribution. Under ideal conditions, each of the powder particles that emerge from the plasma jet, which is carried by the carrier gas, and strikes the substrate would be completely melted. When a spherical liquid droplet hits a flat surface at high velocity, it flattens out into a disc shape and the thin radially projected liquid region becomes unstable and disintegrates into small droplets at the edges [21]. This geometry is also known in the literature as a splat. In plasma spraying, the substrate is at a temperature much lower than the melting point of the molten particle, heat transfer to the substrate is rapid, and the spreading and disintegration of the droplet is stopped by solidification. Finally, the successive deposition of

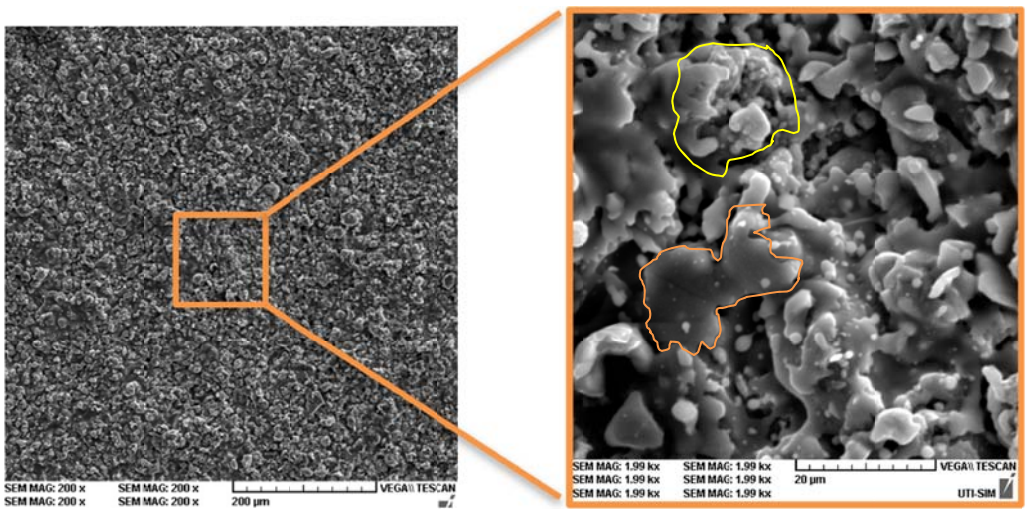

a) b)

Fig. 3. SEI of Cr_2O_3 coating, at various magnification: a) 200×; b) 2000×

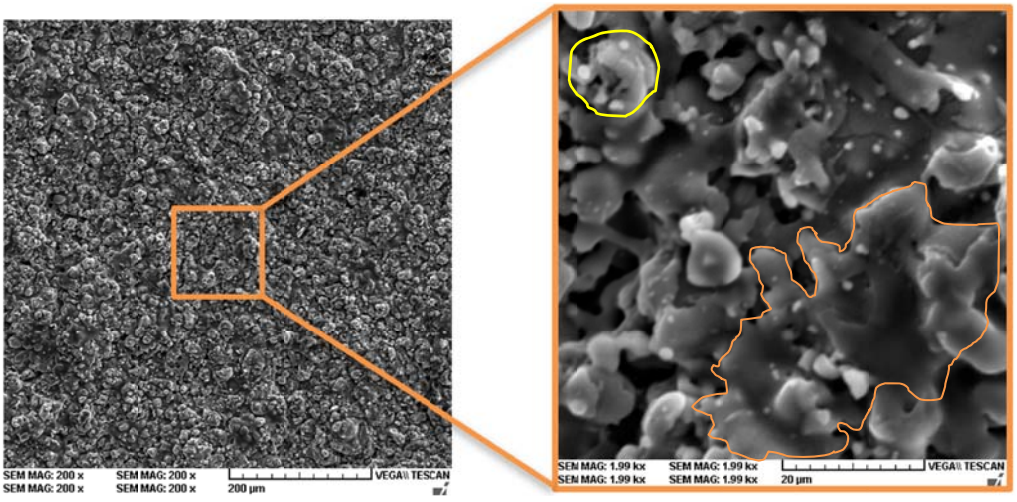

a) b)

Fig. 4. SEI of Cr_2O_3 – 10% TiO_2 coating, at various magnification: a) 200×; b) 2000×

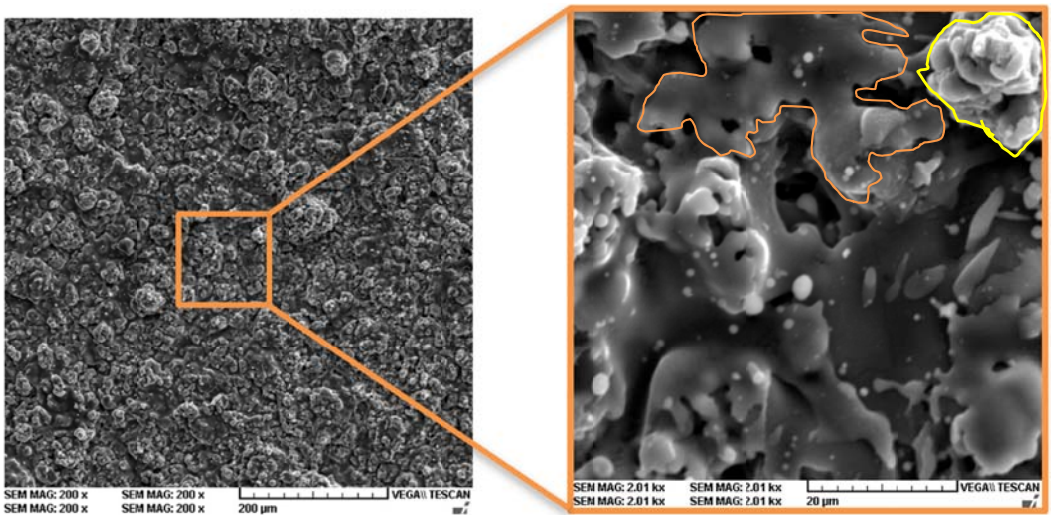

a) b)

Fig. 5. SEI of Cr_2O_3 – 20% TiO_2 coating, at various magnification: a) 200×; b) 2000×

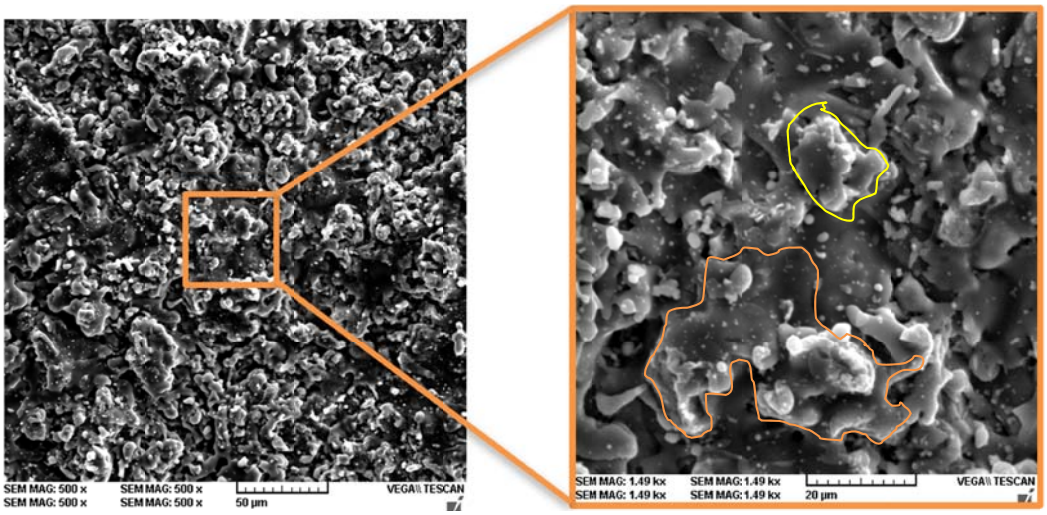

a) b)

Fig. 6. SEI of Cr_2O_3 – 30% TiO_2 coating, at various magnification: a) 200×; b) 2000×

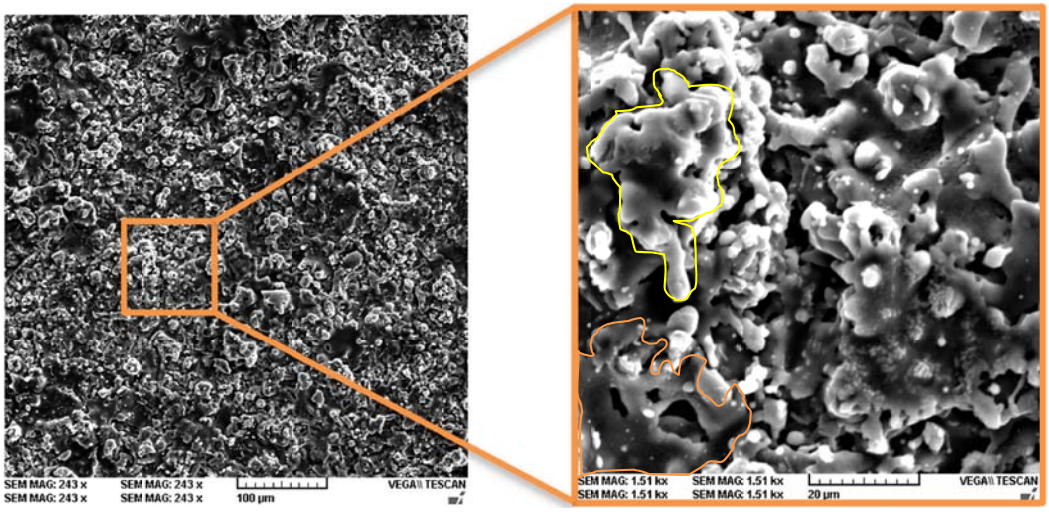

a) b)

Fig. 7. SEI of Cr_2O_3 – 40% TiO_2 coating, at various magnification: a) 200×; b) 2000×

these flattened formations results in a lamellar structure that also contains semi-molten or non-molten particles, voids and oxides of the deposited elements [22].

Starting from this aspect, it can be observed that in all five types of coatings studied, there are formed structures specific to plasma spraying, of splat-by-splat type, being present areas with partially melted particles, but also unmelted [23]. The latter often interfere by reducing the deposition efficiency, as they do not have stable trajectories, while the partially fused ones are incorporated into the coating, modifying the microstructure of the coating and its properties.

At first glance, none of the coatings studied presents major defects, on the surface or at the interface with the substrate, the overall appearance being uniform, without discontinuities or macro cracks.

In Figs. 3a)-7a), realized at magnification powers between 200 and 500×, it can be seen that the porosity of the coatings is determined by the presence of irregular porous formations, obtained due to the imperfect overlapping of splats produced during the deposition process, between which inter and intra-lamellar microcracks are present. Partially melted and solidified particles in coarse granular form can also be observed. These formations are highlighted in Figs. 3b)-7b) by yellow outlining in the case of coarse granular formations and orange outlining in the case of splats.

A comparative analysis of the surfaces in Figs. 3a)-7a) shows that, with the increase in the percentage of TiO_2, there is also an increase in the roughness, i.e. the percentage of coarse particles forming the surface of the coatings studied.

On the images taken in detail, at higher powers between 1500-2000×, the formation of splats, the presence of coarse but fine granular elements, between which voids and microcracks are visible.

3.2. Chemical elements analysis

In addition to the morphological aspects highlighted on the secondary electron images, semi-quantitative elemental chemical analyses, both distribution map and point type, were also performed in some areas of interest for the present study. The distribution map analyses are shown in Figs. 8-12, both in general appearance by superimposing all the elements present on the scanned surface (Figs. 8a)-12a) and individually for each element (Figs. 8-12c,d,e). They are complemented by the graphical representation of the spectra of the elements recorded on the surface and their values in mass percentage, respectively atomic percentage (Figs. 8-12b).

As far as the presence of Ti is concerned, it is observed that, with the increase of the TiO_2 powder mass percentage in the raw material, the areas where it is identified become more numerous, directly proportional to the alloying percentage. For example, on the representative distribution map for the 40%TiO_2 coating a covering of about 50% is observed, which means a good distribution of particles in the spray jet. If we look in the same way at the other distribution maps, compared to the Cr_2O_3 coating map, we observe that for the 10% TiO_2 layer the Ti element is well defined on about 20% of the scanned area (Fig. 9e)), for

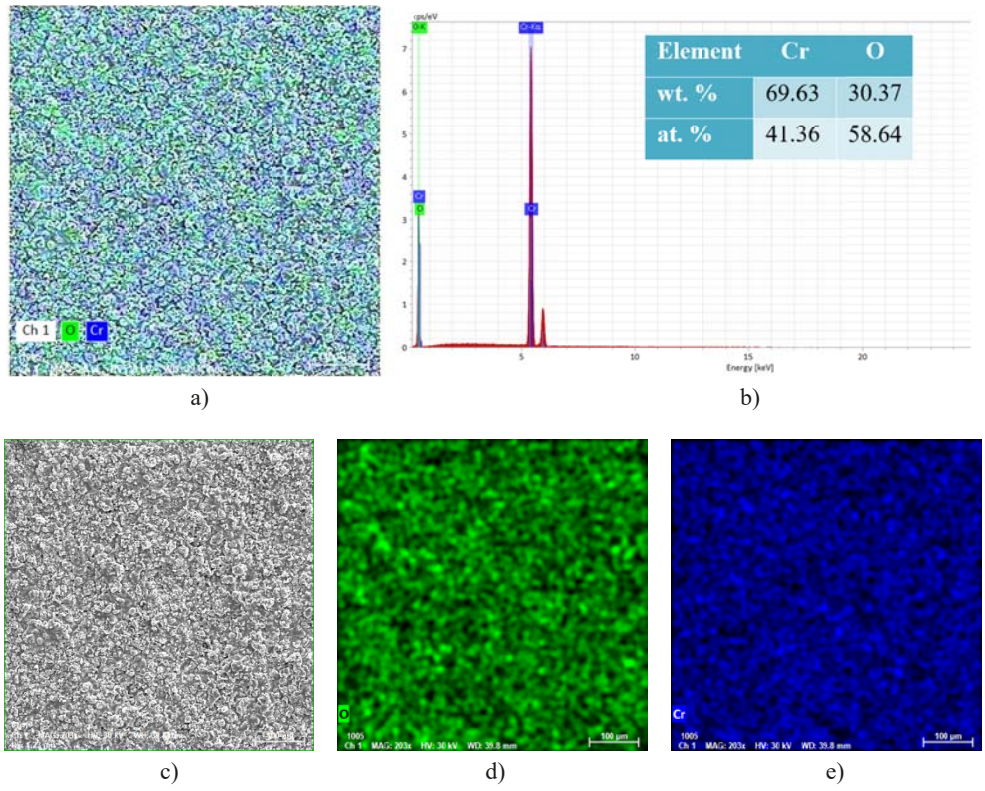

Fig. 8. The chemical composition map of a representative Cr_2O_3 sample area: a) general distribution of all chemical elements from the coating, b) energy dispersive x-ray spectroscopy analysis, c) SEI of the analysed surface, d) O distribution, e) Cr distribution

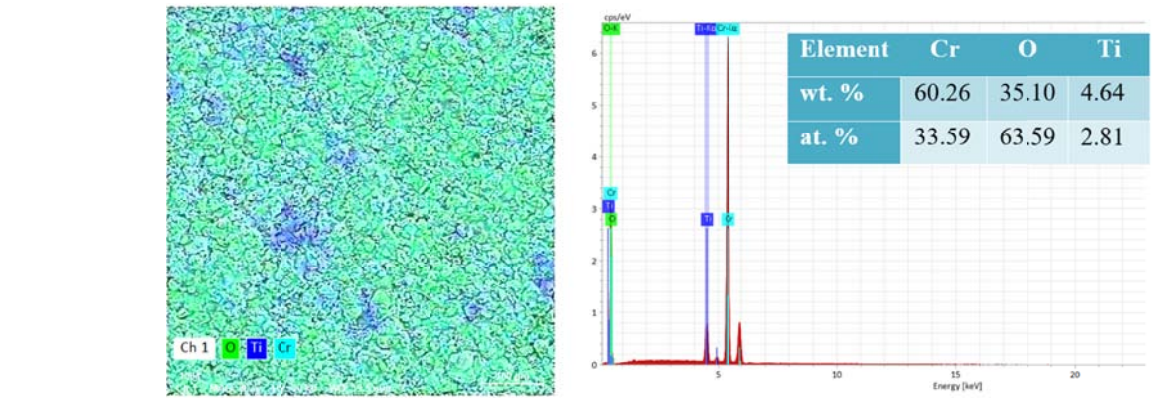

a) b)

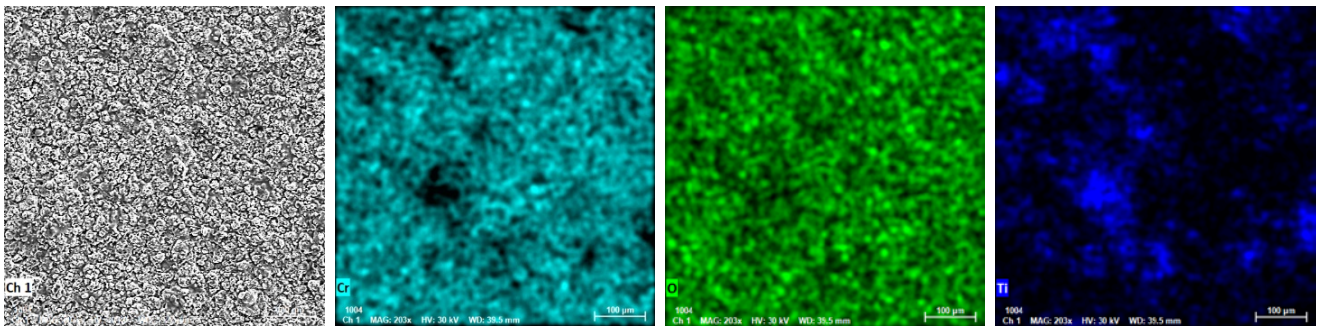

c) d) e) f)

Fig. 9. The chemical composition map of a representative Cr_2O_3 – 10% TiO_2 sample area: a) general distribution of all chemical elements from the coating, b) energy dispersive x-ray spectroscopy analysis, c) SEI of the analysed surface, d) O distribution, e) Cr distribution, f) Ti distribution

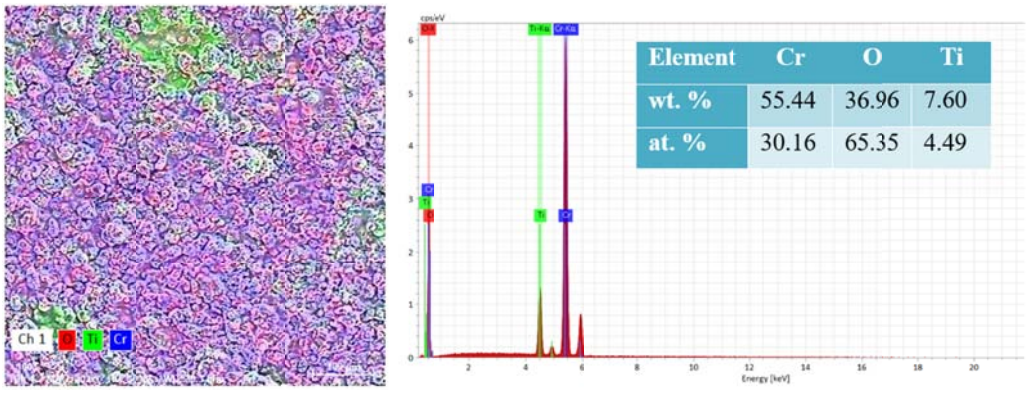

a) b)

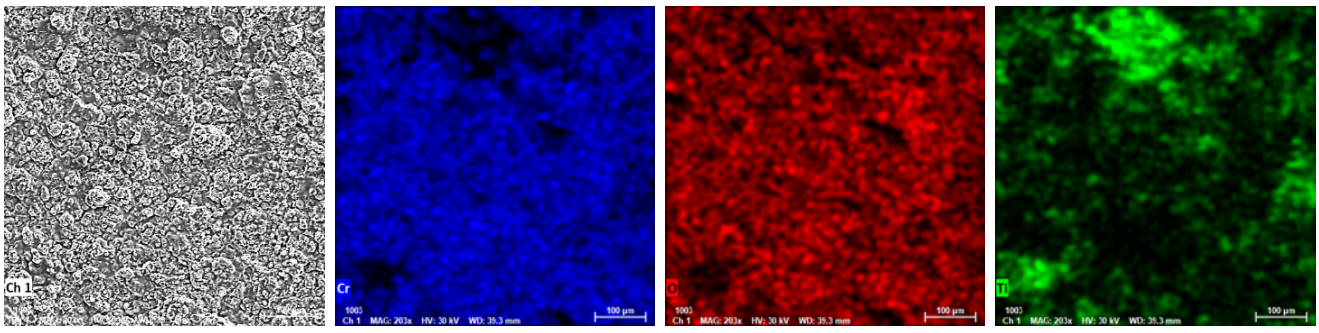

c) d) e) f)

Fig. 10. The chemical composition map of a representative Cr_2O_3 – 20% TiO_2 sample area: a) general distribution of all chemical elements from the coating, b) energy dispersive x-ray spectroscopy analysis, c) SEI of the analysed surface, d) Cr distribution, e) O distribution, f) Ti distribution

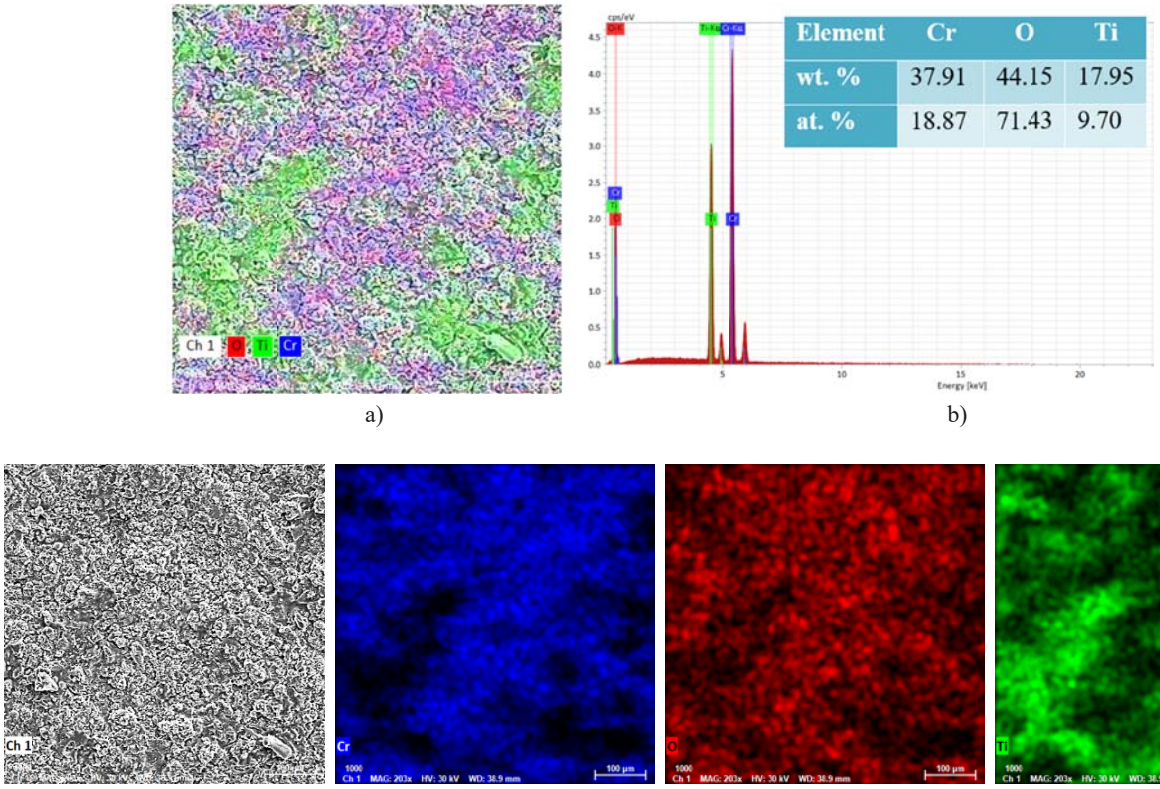

a) b)

c) d) e) f)

Fig. 11. The chemical composition map of a representative Cr_2O_3 – 30% TiO_2 sample area: a) general distribution of all chemical elements from the coating, b) energy dispersive x-ray spectroscopy analysis, c) SEI of the analysed surface, d) Cr distribution, e) O distribution, f) Ti distribution.

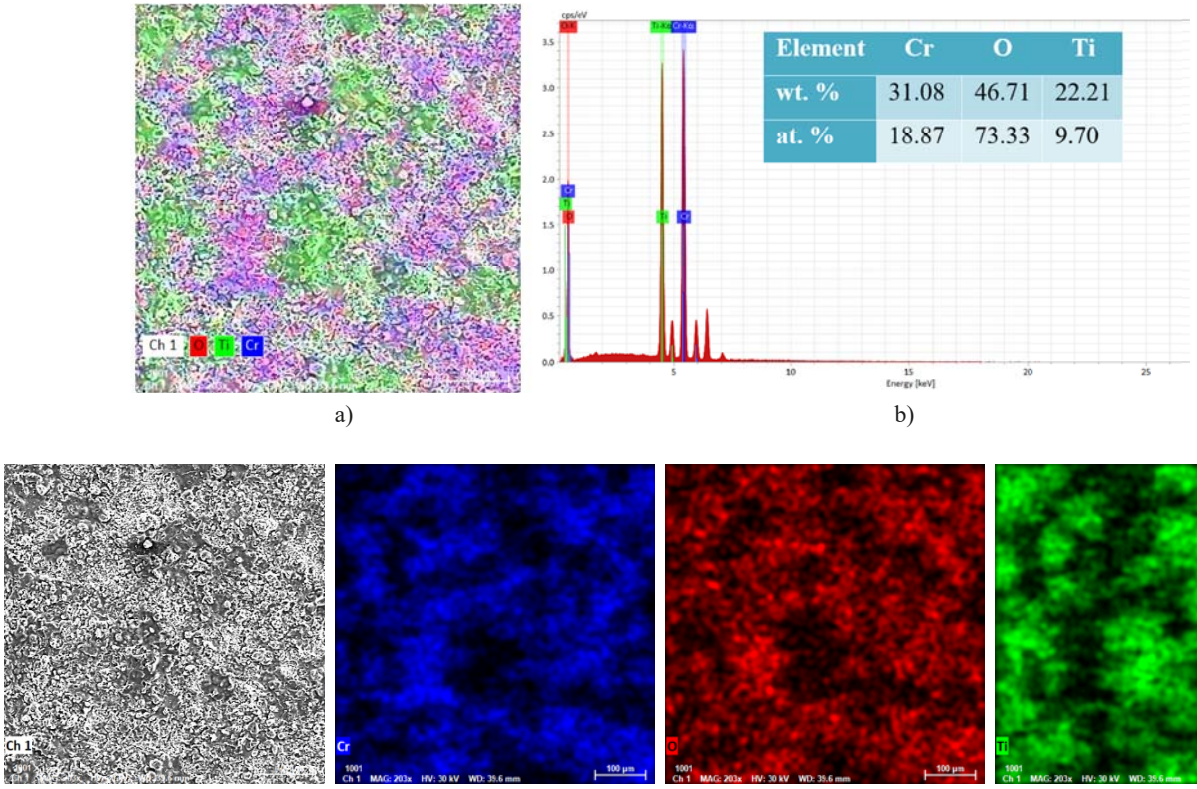

a) b)

c) d) e) f)

Fig. 12. The chemical composition map of a representative Cr_2O_3 – 40% TiO_2 sample area: a) general distribution of all chemical elements from the coating, b) energy dispersive x-ray spectroscopy analysis, c) SEI of the analysed surface, d) Cr distribution, e) O distribution, f) Ti distribution

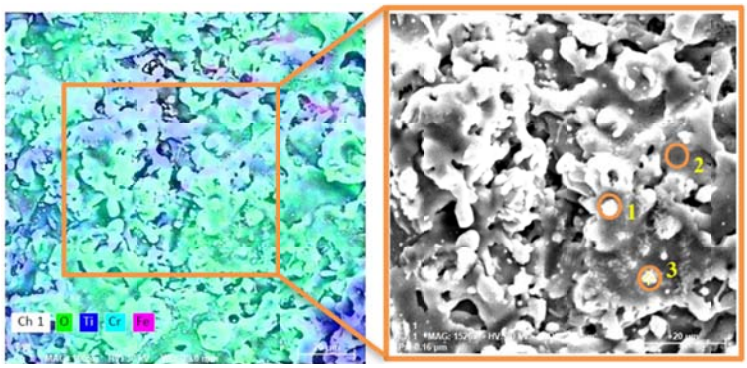

Element		Cr	O	Ti
Point 1	wt. %	47.72	46.03	6.25
	at. %	23.38	73.29	3.33
Point 2	wt. %	39.23	44.88	15.89
	at. %	19.39	72.08	8.53
Point 3	wt. %	64.73	33.97	1.30
	at. %	62.54	36.67	0.80

a) b) c)

Fig. 13. The point chemical composition on a representative area of Cr_2O_3 – 30% TiO_2 sample: a) general distribution of all chemical elements from the coating, b) SEI of the analysed surface (1500×), c) energy dispersive x-ray spectroscopy analysis (table)

the 20% TiO_2 layer the area is about 35% (Fig. 10e)), and for the 30% TiO_2 layer the emission signal from the Ti element is well defined on about 40% (Fig. 11e)). Similarly, an analysis of the other elements found will show that in the areas where the Ti element is present the Cr element is not present, except in the case of the Cr_2O_3 coating, where the uniform distribution of the two chemical elements present, Cr and O, is observed.

At a closer look, we can see that the areas where Ti is present correspond mostly to splat type formations and not to coarse granular ones. This confirms the role of finishing the structure, i.e. increasing the ductility of the ceramic coatings of which the TiO_2 powder is an integral part, by increasing the degree of incorporation of semi-molten or non-molten particles, i.e. by increasing the adhesion between the splats formed during spraying. As can be seen from the distribution maps, the coarse particles are mostly derived from the sprayed Cr_2O_3 particles.

These observations are also confirmed by the point analyses performed on this type of formations marked in Fig. 13, the results of which are shown in Fig. 13c). It is observed that in points 1 and 3 located on a coarse grain (point 1) respectively on a finer grain (point 3) the mass percentage of Cr is very high compared to that of Ti, unlike point 2, located on a splat, where the mass percentage of Ti is about 15%, which means the presence of a titanium-rich compound.

4. Conclusions

In this study, five types of coatings, based on Cr_2O_3 and alloyed with different percentages of TiO_2, were produced by thermal plasma spraying and analysed: 0%, 10%, 20%, 30% and 40% TiO_2. The raw material powder for the 10%, 20% and 30% TiO_2 coatings was obtained by mechanically mixing, in a dry environment, the quantities calculated on the basis of mass percentages, of two commercially available powders: Cr_2O_3 (Amdry 6415, Oerlikon) and Cr_2O_3 40 TiO_2 (Metco 6483, Oerlikon).

The morphological analysis of the produced coatings showed no major defects on the surface or at the interface with the substrate, the overall appearance being uniform, without discontinuities or macrocracks.

On the secondary electron images, taken at magnification powers between 200 and 500×, it is observed that the porosity of the coatings is due to the presence of irregular, coarse granular formations, obtained due to the imperfect overlapping of the splats produced during the deposition process, between which inter and intra-lamellar microcracks are present. The presence of granular formations is directly proportional to the increase of the TiO_2 percentage in the coating, which is also confirmed by EDS analysis performed on the sample surfaces.

Another aspect highlighted by EDS analysis is that Ti is mostly present in splat-type areas, which confirms the role of finishing the structure, i.e. increasing the ductility of the ceramic coatings of which TiO_2 powder is part, by increasing the degree of incorporation of semi-molten or non-molten particles, i.e. by increasing the adhesion between the splats formed during spraying.

However, the percentage of TiO_2 must be limited in the composition of thermal spray coatings, which is why we will carry out additional tests to determine the optimal concentration to achieve the best balance between tribological behaviour, corrosion resistance at high temperatures and low porosity.

REFERENCES

[1] G. Bolelli, D. Steduto, J. Kiilakoski, T. Varis, L. Lusvarghi, P. Vuoristo, Tribological properties of plasma sprayed Cr_2O_3, Cr_2O_3 – TiO_2, Cr_2O_3 – Al_2O_3 and Cr_2O_3 – ZrO_2 coatings. Wear **480-481**, 203931 3203 (2021).

[2] R. Verma, S. Sharma, B. Mukherjee, P. Singh, A. Islam, A.K. Keshri, Microstructural, mechanical and marine water tribological properties of plasma-sprayed graphene nanoplatelets reinforced Al_2O_3- 40 wt% TiO_2 coating. Journal of the European Ceramic Society **42**, 2892-2904 (2022).

[3] J. Viňáš, J. Brezinová, A. Guzanová, Tribological properties of selected ceramic coatings. Journal of Adhesion Science and Technology **27**, 2, 196-207 (2013).
DOI: https://doi.org/10.1080/01694243.2012.701538

[4] S.L. Toma, M. Badescu, I. Ionita, M. Ciocoiu, L. Eva, Influence of the spraying distance and jet temperature on the porosity and

adhesion of the Ti depositions, obtained by thermal spraying in electric arc – Thermal activated. Applied Mechanics and Materials **657**, 296-300 (2014).
DOI: http://dx.doi.org/10.1088/1757-899X/572/1/012056

[5] R.A. Haraga, C. Bejinariu, A. Cazac, B.F. Toma, C. Baciu, S.L. Toma, Influence of surface roughness and current intensity on the adhesion of high alloyed steel deposits-obtained by thermal spraying in electric arc. IOP Conference Series: Materials Science and Engineering **572**, 1, 2, 012056 (2019).
DOI: http://dx.doi.org/10.1088/1757-899X/572/1/012056

[6] S.L. Toma, D.L. Chicet, A.M. Cazac, Numerical Calculation of the Arc-Sprayed Particles' Temperature in Transient Thermal Field. Coatings **12** (7), 877 (2022).
DOI: http://dx.doi.org/10.3390/coatings12070877

[7] C. Park, T. Kim, J. Seol, B. Joshi, A. Aldalbahi, J.-H. Hong, S. An, S. Yoon, Nanotextured surfaces with iron oxide and titania for antibacterial and water purification applications via supersonic spraying. Applied Surface Science **640**, 158376 (2023).

[8] M. Nowakowska, L. Łatka, P. Sokołowski, M. Szala, F.-L. Toma, M. Walczak, Investigation into microstructure and mechanical properties effects on sliding wear and cavitation erosion of Al_2O_3–TiO_2 coatings sprayed by APS, SPS and S-HVOF. Wear **508-509**, 204462 (2022).

[9] D. Lal, S. Sampath, Offset bending for interfacial toughness of plasma sprayed ceramic coatings. Surface & Coatings Technology **469**, 129786 (2023).

[10] P. Ctibor, I. Pis, J. Kotlan, Z. Pala, I. Khalakhan, V. Stengl, P. Homola, Microstructure and Properties of Plasma-Sprayed Mixture of Cr_2O_3 and TiO_2, JTTEE5 **22**, 1163-1169 (2013).
DOI: https://doi.org/10.1007/s11666-013-9969-9

[11] M. Panturu, D. Chicet, S. Lupescu, B. Istrate, C. Munteanu, Applications of ceramic coatings as TBCs on the internal combustion engine valves. Acta Technica Napocensis Series-Applied Mathematics Mechanics and Engineering **61**, 137 (2018).

[12] B. Güney, I. Mutlu, Wear and corrosion resistance of Cr_2O_3 % –40%TiO_2 coating on gray cast-iron by plasma spray technique. Materials Research Express **6**, 9 (2019).
DOI: https://doi.org/10.1088/2053-1591/ab2fb7

[13] C. Paulin, D.L. Chicet, B. Istrate, M. Panturu, C. Munteanu, Corrosion behavior aspects of Ni-base self-fluxing coatings. IOP Conference Series: Materials Science and Engineering **147**, 012034 **(**2016). DOI: http://dx.doi.org/10.1088/1757-899X/147/1/012034

[14] C. Paulin, D. Chicet, V. Paleu, M. Benchea, Ș. Lupescu, C. Munteanu, Dry friction aspects of Ni-based self-fluxing flame sprayed coatings. IOP Conf. Ser. Mater. Sci. Eng. **227**, 012091 (2017).
DOI: http://dx.doi.org/10.1088/1757-899X/227/1/012091

[15] H. Cetinel, E. Celik, M. Kusoglu, Tribological Behavior of Cr_2O_3 Coatings as Bearing Materials. J. Mater. Process. Technol. **196**, 1, 259-265 (2008).
DOI: https://doi.org/10.1016/j.jmatprotec.2007.05.048

[16] T. Varis, J. Knuuttila, T. Suhonen, U. Kanerva, J. Silvonen, J. Leivo, E. Turunen, Improving the Properties of HVOFsprayed Cr_2O_3 by Nanocomposite Powders, Thermal Spray: Crossing Borders, E. Lugscheider, Ed., DVS German Welding Society, 440-443 4 – 9699 (2008).

[17] V.P. Singh, A. Sil, R. Jayaganthan, Tribological behavior of plasma sprayed Cr_2O_3 – 3%TiO_2 coatings. Wear **272**, 149-158, 5485 (2011).

[18] M. Grimm, S. Conze, L.-M. Berger, G. Paczkowski, T.L.T. Lampke, Microstructure and SlidingWear Resistance of Plasma Sprayed Al_2O_3 – Cr_2O_3 – TiO_2 Ternary Coatings from Blends of Single Oxides, Coatings **10**, 42 (2020).
DOI: https://doi.org/10.3390/coatings10010042 0042

[19] L. Bastakys, L. Marcinauskas, M. Milieška, M. Kalin, R. Kezelis, Tribological Properties of Cr_2O_3, Cr_2O_3 – SiO_2 – TiO_2 and Cr_2O_3 – SiO_2 – TiO_2 – Graphite Coatings Deposited by Atmospheric Plasma Spraying. Coatings **13**, 408 (2023).
DOI: https://doi.org/10.3390/coatings 13020408

[20] L. Łatka, M. Szala, M. Nowakowska, M. Walczak, T. Kiełczawa, P. Sokołowski, The effect of microstructure and mechanical properties on sliding wear and cavitation erosion of plasma coatings sprayed from Al2O3 + 40 wt% TiO2 agglomerated powders. Surface & Coatings Technology **455**, 129180 (2023).

[21] C.C. Paleu, C. Munteanu, B. Istrate, S. Bhaumik, P. Vizureanu, M.S. Bălţatu, V. Paleu, Microstructural Analysis and Tribological Behavior of AMDRY 1371 (Mo–NiCrFeBSiC) Atmospheric Plasma Spray Deposited Thin Coatings. Coatings **10**, (12), 1186 (2020).
DOI: http://dx.doi.org/10.3390/coatings10121186

[22] B. Istrate, C. Munteanu, S. Lupescu, M. Benchea, P. Vizureanu, Preliminary Microstructural and Microscratch Results of Ni-Cr-Fe and Cr_3C_2-NiCr Coatings on Magnesium Substrate. IOP Conference Series: Materials Science and Engineering **209**, 012024 (2017). DOI: http://dx.doi.org/10.1088/1757-899X/209/1/012024

[23] D. Chicet, A. Tufescu, C. Paulin, M. Panturu, C. Munteanu, The Simulation of Point Contact Stress State for APS Coatings. IOP Conference Series: Materials Science and Engineering **209** (1), art. no. 012044 (2017).